

Laser spinning of nanotubes: A path to fast-rotating microdevices

Petr Král^{1,2} and H. R. Sadeghpour²

¹Department of Chemical Physics, Weizmann Institute of Science, 76100 Rehovot, Israel

²ITAMP, Harvard-Smithsonian Center for Astrophysics, Cambridge, Massachusetts 02138

(Received 15 January 2002; published 29 March 2002)

We show that circularly polarized light can spin nanotubes with GHz frequencies. In this method, angular momenta of infrared photons are resonantly transferred to nanotube phonons and passed to the tube body by “Umklapp” scattering. We investigate experimental realization of this ultrafast rotation in carbon nanotubes, levitating in an optical trap and undergoing mechanical vibrations, and discuss possible applications to rotating microdevices.

DOI: 10.1103/PhysRevB.65.161401

PACS number(s): 32.80.Lg, 62.25.+g, 78.67.Ch, 85.35.Kt

Carbon nanotubes¹ have unique mechanical and electronic properties with many potential applications.² They possess a huge Young’s modulus $Y > 1$ TPa, which adjusts their autonomous mechanical oscillations to MHz frequencies.³ Moreover, their “molecular structures” remain naturally stable even at large deformations.⁴

Therefore, rotationally symmetric structures based on stiff nanotubes could form ideal *piston rods* for nanoscale applications. In contrast to chemically driven biomotors,⁵ spinning with Hertz frequencies, such tubular structures could rotate very fast, if angular momentum is efficiently transferred to them and friction is reduced.

Small heteropolar molecules can be dissociated,⁶ if *synchronously* rotated with a dipolar laser trap, which accelerates its angular velocity. Larger molecules⁷ and microparticles⁸ can be rotated by absorption of angular momentum from circularly polarized or “twisted” laser beams. Nanotubes are excellent candidates for this *asynchronous* driving, where the system rotational frequency is much smaller than the light frequency.

Here, we investigate ultrafast asynchronous rotation induced in nanotubes by excitation of their *vibrational* modes with circularly polarized light. The mode selection is restricted by radiational heating, since each photon absorbed by the tube transfers to it angular momentum \hbar and energy $\hbar\omega$. The resulting heating can be limited in excitation of infrared (IR) A_{2u} or E_{1u} phonon modes, active in graphite⁹ and nanotubes.¹⁰

In Fig. 1 we show two schemes for spinning nanotubes. In the upper one, circularly polarized light beam propagates along the symmetry axis of the single-wall nanotube (SWNT) or multiwall nanotube (MWNT), levitating in an optical trap. The photon angular momentum is transferred to *circularly polarized* phonons, counterpropagating on the tube circumference (see Fig. 2), and latter passed by scattering to the tube body. The angular momentum of light could be also directly passed to the nanotube in excitation of its dense rotational levels. The resulting tube rotation with angular frequency ω_{rot} is mostly balanced by friction with the surrounding molecules. In the lower configuration, a closed nanotube ring¹¹ is analogously rotated by absorption of circularly polarized photons.

We can describe the excitation of nanotube phonons by circularly polarized light, and the subsequent relaxation, with the simplified Hamiltonian

$$H = \sum_{\alpha} \hbar \omega_{\alpha} b_{\alpha}^{\dagger} b_{\alpha} + \sum_{\alpha_{\pm}} \mu_{\alpha_{\pm}} E^{\pm}(t) (b_{\alpha_{\pm}}^{\dagger} + b_{\alpha_{\pm}}) + \sum_{\alpha_{\pm}, \beta, \gamma} (c_{\alpha_{\pm}, \beta, \gamma} b_{\alpha_{\pm}}^{\dagger} b_{\beta} b_{\gamma} + \text{H.c.}) + H_d. \quad (1)$$

The first two terms describe phonon modes $\alpha = (\text{band}, k)$ and coupling of the chosen IR circularly polarized optical phonons, with operators¹² $b_{\alpha_{\pm}}^{\dagger} = 2^{-1/2}(b_{\alpha x}^{\dagger} \pm i b_{\alpha y}^{\dagger})$ and $b_{\alpha_{\pm}} = 2^{-1/2}(b_{\alpha x} \mp i b_{\alpha y})$, to the light intensity $E^{\pm}(t)$ of the same polarization. The third term denotes decay of these IR phonons, with wave vectors $k \approx 0$, into phonon pairs with opposite wave vectors $\pm k$, which most likely come from the same acoustical branch.^{13,14} These also cannot carry angular quasimomentum L , which is passed to the tube by Umklapp processes. The resulting tube rotation is predominantly damped by scattering with molecules, as described in H_d .¹⁵

In Fig. 2, we show two (doubly degenerate) IR modes in the elementary cell, with 40 atoms, of the (10,10) nanotube. In the A_{2u} and E_{1u} modes, the atoms move out of plane and in plane, respectively, orthogonal to the tube axis,¹⁶ as shown by open circles. Combination of the two degenerate linearly polarized modes form a *circularly polarized* phonon mode,

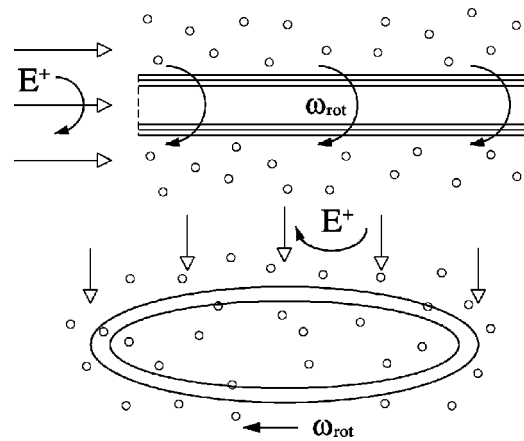


FIG. 1. Scheme for nanotube (up) and tubular ring (down) spinning with angular velocity ω_{rot} in a laser trap. Their rotation is induced by absorption of circularly polarized photons from a laser beam with intensity E^+ , propagating along the axis of rotational symmetry. Scattering of molecules with tubes damps the rotation.

of either symmetry, which can absorb angular quasimomentum from circularly polarized photons. The atomic displacements break the tube symmetry and induce electric dipoles (+ −), which follow in time the polarization of the circulating electric field \mathbf{E}^+ . The effect does not rely on coherent light and can be also realized in tubular rings (see Fig. 1).

As an example, we consider excitation of the A_{2u} mode. The total number $n_{A_{2u}}^+$ of circularly polarized phonons, excited in the vicinity of $k=0$, is given by the Boltzmann equation

$$\frac{\partial n_{A_{2u}}^+}{\partial t} = \dot{n}_{A_{2u}}^+ - \frac{n_{A_{2u}}^+ - n_{A_{2u}}^{+,equil.}}{\tau_{A_{2u}}}. \quad (2)$$

$\dot{n}_{A_{2u}}^+$ is their injection rate and $\tau_{A_{2u}} = 2\hbar/\gamma_{A_{2u}} \approx 2$ ps, is the relaxation time, where $\gamma_{A_{2u}} \approx 22$ cm^{-1} is the width of the IR phonon lines in nanotubes.¹⁰ We neglect small populations $n_{A_{2u}}^-$ of phonons with the opposite polarization, resulting in scattering.

The absorption line of the A_{2u} (E_{1u}) mode was observed near $\omega_{A_{2u}} = 870$ cm^{-1} (1580 cm^{-1}) in both graphite and C nanotubes. In graphite, the A_{2u} mode has an oscillator strength⁹ $f \approx 0.004$, which we assume to approximately hold in C nanotubes. Its optical dipole moment is¹⁷ $\mu_{A_{2u}} = e\sqrt{3\hbar f/2m_{osc}\omega_{A_{2u}}} \approx 10^{-31}$ Cm, where $m_{osc} = M_{Carbon}/2$ is the oscillator mass. Using the Fermi's golden rule, and assuming that $n_{A_{2u}}^{+,equil.} \approx 0$, we obtain the injection rate

$$\dot{n}_{A_{2u}}^+ \approx \frac{2\pi}{\hbar} |\mu_{A_{2u}} E^+|^2 \rho(\omega_{A_{2u}}), \quad (3)$$

where $\rho(\omega_{A_{2u}})$ is the density of phonon modes at $k=0$. An armchair (10,10) nanotube of length $l=1$ μm has $n \approx 1.6 \times 10^5$ C atoms and $N=n/40=4000$ elementary cells (A_{2u} modes with $k \neq 0$). About 10% of these modes (around $k=0$) fall in the energy window $\gamma_{A_{2u}}$, thus giving the effective mode density $\rho(\omega_{A_{2u}}) \approx 400/\gamma_{A_{2u}}$. For a field strength $E^+ = 10$ kV/m, we then obtain from Eq. (3) that $\dot{n}_{A_{2u}}^+ \approx 2.5 \times 10^5$ s^{-1} . The IR phonons thus absorb the angular quasimomentum with the rate $\dot{L}_{A_{2u}} = \hbar \dot{n}_{A_{2u}}^+ \approx 2.5 \times 10^{-29}$ Nm.

We can understand the angular quasimomentum Umklapp processes by unrolling the nanotube, and loosely binding many such sheets into a superlattice of lattice constant $a_s = 2\pi r$, where r is the tube diameter. Then, the IR phonons have the transversal wave vector $K_0 = 2\pi/a_s$, which falls in the middle of the second Brillouin minizone of size $Q = K_0$. In a two-phonon Umklapp decay, the momentum conservation is $K_0 + K_1 + K_2 = Q$ (transversal wave vectors of the decayed acoustical phonons are $K_{1,2}=0$), where the vector Q interconnects centers of the first and second minizone. In the nanotube, we can vector multiply this identity by $\hbar r$, and obtain the (Umklapp) angular quasimomentum conservation $L_0 + L_1 + L_2 = \hbar Q \times r$ ($L_{1,2}=0$), where $L_0 = \hbar K_0 \times r = \hbar$.

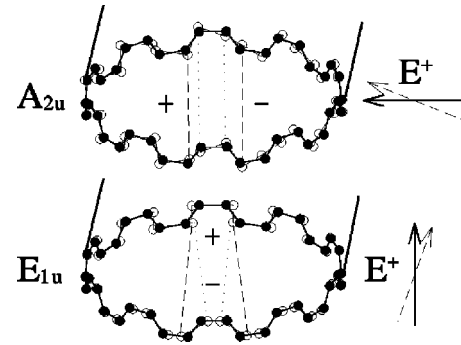


FIG. 2. Nanotube cross sections with light-induced atomic displacements (open circles) from equilibrium positions (filled circles) in two IR phonon modes, with the A_{2u} and E_{1u} symmetries. A circularly polarized light, \mathbf{E}^+ , excites phonon waves, which propagate unidirectionally on the tube circumference in phase with the light polarization.

In Eq. (2) these processes are represented by the relaxation time $\tau_{A_{2u}}$, which could be derived from Eq. (1) following Klemens.¹³ Its experimental value, $\tau_{A_{2u}} \approx 2$ ps, is in agreement with decay times of the suggested processes realized in other systems.¹⁴ Since *ab initio* calculations of the phonon matrix elements $c_{\alpha\pm,\beta,\gamma}$ are lacking, we use this value of $\tau_{A_{2u}}$ in our modeling. Equation 2 then gives the steady-state angular quasimomentum in the A_{2u} phonon bath $L_{A_{2u}} = \hbar \Delta n_{A_{2u}}^+ = \dot{L}_{A_{2u}} \tau_{A_{2u}} \approx 5.2 \times 10^{-41}$ Js.

The angular momentum is transferred to the tube body at the rate $\dot{L} \approx \dot{L}_{A_{2u}}$. Nanotubes in liquids¹⁵ or under atmospheric conditions would rotate slowly, since collisions with the surrounding molecules quickly dissipate the acquired angular momentum. On the other hand, in low-vacuum environment, with realistic collisional rates $\kappa \approx 10^{-12} - 10^{-13}$ $\text{cm}^3 \text{s}^{-1}$, damping times of the order $\tau_{damp} \approx 10$ s are readily achievable. The tube thus keeps a steady-state angular momentum $L \approx \dot{L}_{A_{2u}} \tau_{damp} \approx 2.5 \times 10^{-28}$ Js.

The nanotube rotation frequency ω_{rot} can be found upon calculating its principal moments of inertia¹⁸⁻²⁰

$$A = B = M \left(\frac{r_e^2 + r_i^2}{4} + \frac{l^2}{12} \right), \quad C = M \frac{r_e^2 + r_i^2}{2}. \quad (4)$$

Here $M = \rho l$, r_e , r_i , and l are the nanotube mass (ρ is the linear density), exterior and interior radii, and length, respectively. For the (10,10) armchair nanotube with $r = (r_e + r_i)/2 \approx 0.68$ nm and $l = 1$ μm , we obtain $M \approx 1.9 \times 10^{-20}$ kg and $A \approx 1.6 \times 10^{-33}$ kg $\text{m}^2 \approx 1.8 \times 10^5 C$.

Finally, we find the rotation speed $\omega_{rot} = L/C \approx 28$ GHz for this elementary nanomechanical device. Centrifugal acceleration on its surface is enormous, $a = r\omega_{rot}^2 = 0.5 \times 10^{12}$ $\text{m/s}^2 \approx 10^{11}g$. This value surpasses by two orders of magnitude the acceleration obtained with sub-millimeter steel balls,²¹ and by five orders of magnitude acceleration in the fastest centrifuges.²² Since for $a = 10^{11}g$, the force on each C atom, $F \approx 13$ $\mu\text{eV}/\text{\AA}$ is still negligible with respect to chemical forces (1 eV/ \AA), the tube rotation could be

further increased. On this path to “teragravity,” unique parameters of nanotubes can play a pivotal role.

We can now discuss in more details practical spinning experiments. Isolated SWNT or MWNT have been grown, for example, on an atomic force microscope tip,²³ which can be later placed inside an optical trap. The nanotube can be severed from the tip using, for instance, a focused electron beam.²⁴ Detached tubes could be also transported to the trap by recently developed nanotweezers.²⁵ The optical trap can be formed by two linearly and mutually parallel polarized, counterpropagating laser beams.²⁶

Nonresonant scattering of trap-beam photons from the nanotube with polarizability α produces a force, oriented in the direction of increasing light intensity I , that results in the potential $U = -\alpha I/2c$ (c is the speed of light). The longitudinal $\alpha_{zz} \approx 500 \text{ \AA}^3/\text{atom}$ and radial $\alpha_{xx} \approx 25 \text{ \AA}^3/\text{atom}$ static polarizabilities of semiconducting nanotubes²⁷ are quite different, and this difference is even larger in metallic tubes. Therefore, the tube in the trap remains oriented along the beam polarization axis, where it experiences the trapping potential

$$U \approx -U_0 e^{-(r^2/\sigma_r^2 - z^2/\sigma_z^2)} \approx -(U_0 - S r^2) e^{-z^2/\sigma_z^2}. \quad (5)$$

Here x, y, z ($r = x^2 + y^2$) are the tube center-of-mass coordinates, and $S = S_0 l = U_0 / \sigma_r^2$ is the trap rigidity. To prevent thermal escape of the tube from the trap, we consider a trap depth $U_0 = n \alpha_{zz} I / 2c \approx 10 \text{ eV}$, and obtain $I \approx 1.2 \text{ GW/cm}^2$. The trap laser frequency must be below the band gap $E_g \approx 1 \text{ eV}$, and away from the frequencies of the tube internal modes, see below. Assuming that $\sigma_r \approx 1 \text{ }\mu\text{m}$, we find $S_0 = U_0 / l \sigma_r^2 \approx 1.6 \text{ J/m}^3$.

Small amounts of defects and adsorbants on the tube walls do not prevent its spinning, but can shift its rotation frequency. In accordance with the De Laval principle of self-balancing,²⁰ such a partially coated nanotube floating in the trap would rotate around an eccentric axis. Rapid rotation of the nanotube can be also limited by its mechanical vibrations in the trap, as discussed below. To avoid its large oscillations, the critical frequencies should be quickly passed during the acceleration.^{19,20}

The *cylindrical* whirl mode²⁰ reflects the rigid-body vibrations of the tube orthogonal to the trap axis. The forward (backward) cylindrical frequencies are $\omega_{cyl} = \pm \sqrt{S_0 / \rho} \approx \pm 9.2 \text{ MHz}$. In the *conical* whirl mode, the tube ends move in opposite directions with respect to the tube/trap axis. For a tube distorted through the angle θ , the torsional moment is $M_F \approx -S_0 l^3 \theta / 6$, resulting in the Euler’s equation,¹⁹ $A \omega_{con}^2 = C \omega_{rot} \omega_{con} + S_0 l^3 / 6$. Using $A \approx \rho l^3 / 12$, valid for $l \gg r$, we obtain

$$\omega_{con} = \frac{C \omega_{rot}}{2A} \pm \sqrt{\left(\frac{C \omega_{rot}}{2A}\right)^2 + \frac{2S_0}{\rho}}. \quad (6)$$

We can see that the modal frequencies depend on ω_{rot} due to *gyroscopic* effects.²⁰ Since the ratio $C/A \approx l^{-2}$ is small, the effects are suppressed by the potential U , so that $\omega_{con} \approx \sqrt{2} \omega_{cyl}$. From Eq. (6), we find that they begin to play a role for tube lengths $l < (r_e + r_i) \sqrt{3} \omega_{rot} / \omega_{cyl} \approx 130 \text{ nm}$. If

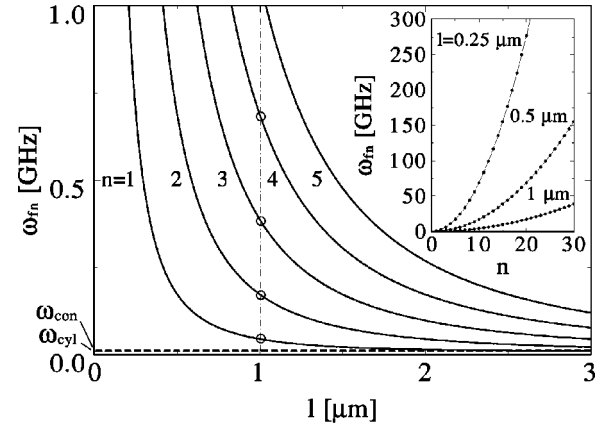


FIG. 3. Dependence of the critical flexural frequencies ω_{fn} on the nanotube length l . The two thin horizontal dashed lines correspond to ω_{cyl} and ω_{con} . In the inset, we show ω_{fn} as a function of the bending modal number n for nanotubes of different length.

the trap is suddenly switched off, a micron-long nanotube rotating with frequency $\omega_{rot} = 28 \text{ GHz}$, and initially disturbed on its side, would precess with the frequency $\omega_{prec} = C \omega_{rot} / A \approx 175 \text{ kHz}$.

In long nanotubes, one needs to consider also *flexural* vibrations.^{18–20} The critical flexural frequencies ω_f can be evaluated from the equations for lateral deflections $x(z)$, $y(z)$ at different points z along the trap axis, if the rigid-body approximation is abandoned. The equation for the x deflection is

$$YI \frac{\partial^4 x}{\partial z^4} = -\rho \frac{\partial^2 x}{\partial t^2} - S_0 x + a \frac{\partial^2}{\partial t^2} \left(\frac{\partial^2 x}{\partial z^2} \right) + c \omega_{rot} \frac{\partial}{\partial t} \left(\frac{\partial^2 y}{\partial z^2} \right). \quad (7)$$

Here Y is the Young’s modulus, $I = \pi(r_e^4 - r_i^4)/4$ is the second moment of nanotube cross section, and the factors $c = 2a = \rho(r_e^2 + r_i^2)/2$ are the densities of the moments of inertia,¹⁹ which correspond to the bulk expressions in Eq. (4) in the limit $l \rightarrow 0$. The equation for the y deflection results from Eq. (7) by exchanging $x \leftrightarrow y$ and a negative sign in the last term.

The flexural frequencies correspond to the solutions $x = x_0 \cos(\omega_f t)$, $y = y_0 \sin(\omega_f t)$ in Eq. (7). This substitution gives an ordinary differential equation, identical for both the x and y deflections. For simplicity, we apply the clamped-end approximation, with the boundary conditions $x_0(z = \pm l/2) = d^2 x_0(z = \pm l/2) / dz^2 = 0$. The solutions are $x_0(z) = A_0 \cos(\xi z)$ or $x_0(z) = A_0 \sin(\xi z)$, where $\xi^2 = (\alpha + \sqrt{\alpha^2 - 4\beta YI}) / 2YI$, $\alpha = a \omega_f^2 - c \omega_{rot} \omega_f$, and $\beta = S_0 - \rho \omega_f^2$. Therefore, $\xi = n \pi / l$, with $n = 1, 2, 3, \dots$ indexing the eigenmodes, which leads to the *critical* flexural frequencies ($\omega_{fn} = \omega_{rot}$)

$$\omega_{fn} = \sqrt{\frac{S_0 / \rho + (n \pi / l)^4 YI / \rho}{1 - (n \pi r / l)^2 / 2}}. \quad (8)$$

We use the values $Y \approx 5.5 \text{ TPa}$ and $h = r_e - r_i = 0.066 \text{ nm}$, found in molecular-dynamics simulations.²⁸

In Fig. 3, we show the dependence of the lowest critical

frequencies ω_{fn} on the tube length l , calculated from Eq. (8) using the numerical values for Y , h , ρ , S_0 , and r . For long tubes, the frequencies ω_{fn} coincide with ω_{cyl} , while for shorter tubes ($l < 1.3 \mu\text{m}$), the bending term surpasses the trap term, and $\omega_{fn} = (n\pi/l)^2 \sqrt{YI/\rho}$. In the continuum description, gyroscopic effects become only important for high eigenmodes $n \approx l/r$. In the inset of Fig. 3, we also show the dependence of ω_{fn} on n for tubes of different lengths. The huge Young's modulus Y makes the density of critical frequencies ω_{fn} relatively low, especially for short nanotubes. This allows for a rapid traversal to the "supercritical state," which is realized above the flexural or other vibrational frequencies.

Rotating nanotubes could form parts of nanomotors, centrifuges or stabilizers. Centrifugal studies could be performed inside microtubes with large diameters $d \approx 10 \mu\text{m}$

(Ref. 29) or in assemblies made from nanotube rings, forming strong but flexible skeletal coats. One could also think about possible applications of rotating tubes in liquids. Slowly rotating coiled nanotubes³⁰ could, for example, propel microscopic systems, which would chemically power the rotation of these tubes that attached to their surfaces in bearings,³¹ as in biomotors. We believe that unique properties of nanotubes made from carbon and other materials could foster applications with rotating microelements.

We would like to thank R. Saito and G. Dresselhaus for data on IR phonon modes and several useful discussions. P.K. would like to acknowledge support from EU COCOMO. This work was also supported by the US National Science Foundation through a grant to the Institute for Theoretical Atomic and Molecular Physics at the Harvard-Smithsonian Center for Astrophysics.

-
- ¹S. Iijima, *Nature (London)* **354**, 56 (1991).
²M.S. Dresselhaus, G. Dresselhaus, and P.C. Eklund, *Science of Fullerenes and Carbon Nanotubes* (Academic Press Inc., San Diego, 1996).
³M.M. Treacy, T.W. Ebbesen, and J.M. Gibson, *Nature (London)* **381**, 678 (1996); R. Gao *et al.*, *Phys. Rev. Lett.* **85**, 622 (2000).
⁴O. Lourie, D.M. Cox, and H.D. Wagner, *Phys. Rev. Lett.* **81**, 1638 (1998).
⁵D. Walz and S.R. Caplan, *Biophys. J.* **78**, 626 (2000); F.A. Samatey *et al.*, *Nature (London)* **410**, 331 (2001).
⁶J. Karczmarek, J. Wright, P. Corkum, and M. Ivanov, *Phys. Rev. Lett.* **82**, 3420 (1999); D.M. Villeneuve *et al.*, *ibid.* **85**, 542 (2000).
⁷E. Santamato, B. Daino, M. Romagnoli, M. Settembre and Y.R. Shen, *Phys. Rev. Lett.* **57**, 2423 (1986).
⁸E. Higurashi *et al.*, *Appl. Phys. Lett.* **64**, 2209 (1994); L. Paterson *et al.*, *Science* **292**, 912 (2001).
⁹R.J. Nemanich, G. Lucovsky, and S.A. Solin, *Solid State Commun.* **23**, 117 (1977).
¹⁰J. Kastner *et al.*, *Chem. Phys. Lett.* **221**, 53 (1994); U. Kuhlmann, H. Jantoljak, N. Pfander, P. Bernier, C. Journet, and C. Thomsen, *ibid.* **294**, 237 (1998).
¹¹J. Liu *et al.*, *Nature (London)* **385**, 780 (1997).
¹²A.A. Kiselev, *Opt. Spectrosc.* **53**, 469 (1982).
¹³P. G. Klemens, in *Solid State Physics*, edited by F. Seitz and D. Turnbull (Academic Press Inc., NY, 1958), Vol. 7; P.G. Klemens, *Phys. Rev.* **148**, 845 (1966).
¹⁴S. Usher and G.P. Srivastava, *Phys. Rev. B* **50**, 14 179 (1994).
¹⁵P. Král and M. Shapiro, *Phys. Rev. Lett.* **86**, 131 (2001).
¹⁶R. Saito (private communication).
¹⁷R.W. Boyd, *Nonlinear Optics* (Academic Press, New York, 1992).
¹⁸L.D. Landau and E.M. Lifshitz, *Elasticity Theory* (Pergamon, Oxford, 1986).
¹⁹R.N. Arnold and L. Maunder, *Gyrodynamics and its Engineering Applications* (Academic, NY, 1961).
²⁰S. Whitley, *Rev. Mod. Phys.* **56**, 41 (1984); *ibid.* **56**, 67 (1984).
²¹J.W. Beams, *Sci. Am.* **204**, 134 (1961).
²²T. Mashimo, S. Okazaki, and S. Shihabazaki, *Rev. Sci. Instrum.* **67**, 3170 (1996).
²³Ch.L. Cheung, J.H. Hafner, T.W. Odom, K. Kim, and C.M. Lieber, *Appl. Phys. Lett.* **76**, 3136 (2000).
²⁴S. Trasobares *et al.*, *Eur. Phys. J. B* **22**, 117 (2001).
²⁵P. Kim and C.M. Lieber, *Science* **286**, 2148 (1999).
²⁶A. Ashkin, *Phys. Rev. Lett.* **24**, 156 (1970); M.J. Renn, R. Pastel, and H.J. Lewandowski, *ibid.* **82**, 1574 (1999).
²⁷L.X. Benedict, S.G. Louie, and M.L. Cohen, *Phys. Rev. B* **52**, 8541 (1995).
²⁸B.I. Yakobson, C.J. Brabec, and J. Bernholc, *Phys. Rev. Lett.* **76**, 2511 (1996).
²⁹M. Remškar *et al.*, *Appl. Phys. Lett.* **69**, 351 (1996).
³⁰X.B. Zhang *et al.*, *Europhys. Lett.* **27**, 141 (1994); A. Volodin *et al.*, *Phys. Rev. Lett.* **84**, 3342 (2000).
³¹A.N. Kolmogorov and V.H. Crespi, *Phys. Rev. Lett.* **85**, 4727 (2000); J. Cumings and A. Zettl, *Science* **289**, 602 (2000).